

In Vivo Imaging and Noninvasive Ablation of Pyramidal Neurons in Adult *NEX-CreERT2* Mice

Amit Agarwal^{1,2}, Payam Dibaj¹, Celia M. Kassmann¹, Sandra Goebbels¹, Klaus-Armin Nave¹ and Markus H. Schwab¹

¹Department of Neurogenetics, Max Planck Institute of Experimental Medicine, 37075 Goettingen, Germany

²Current address: The Solomon H. Snyder Department of Neuroscience, Johns Hopkins University, Baltimore, Maryland 21205, USA

Address correspondence to Dr Klaus-Armin Nave, Department of Neurogenetics, Max Planck Institute of Experimental Medicine, Hermann-Rein-Strasse 3, 37075 Goettingen, Germany. Email: nave@em.mpg.de

To study the function of individual neurons that are embedded in a complex neural network is difficult in mice. Conditional mutagenesis permits the spatiotemporal control of gene expression including the ablation of cells by toxins. To direct expression of a tamoxifen-inducible variant of Cre recombinase (CreERT2) selectively to cortical neurons, we replaced the coding region of the murine *Nex1* gene by CreERT2 cDNA via homologous recombination in embryonic stem cells. When injected with tamoxifen, adult *NEX-CreERT2* mice induced reporter gene expression exclusively in projection neurons of the neocortex and hippocampus. By titrating the tamoxifen dosage, we achieved recombination in single cells, which allowed multiphoton imaging of neocortical neurons in live mice. When hippocampal projection neurons were genetically ablated by induced expression of diphtheria toxin, within 20 days the inflammatory response included the infiltration of CD3+ T cells. This marks a striking difference from similar studies, in which dying oligodendrocytes failed to recruit cells of the adaptive immune system.

Keywords: connectivity, Cre knock-in, hippocampus, pyramidal cells, tamoxifen

Introduction

Glutamatergic pyramidal neurons constitute the majority of neurons in the mammalian hippocampus and neocortex (Nieuwenhuys 1994), participating in large neuronal networks that are the basis for higher brain functions. The perturbation or physical degeneration of cortical pyramidal neurons and their processes is associated with severe neurological and psychiatric disorders, including Alzheimer's disease (Morrison and Hof 1997). While the morphological features of cortical projection neurons are known for more than 100 years (reviewed in DeFelipe and Farinas 1992; Spruston 2008) and also transgenic and viral labeling techniques have been used to trace the neuronal morphology (Dittgen et al. 2004), it remains difficult to combine the morphology and function of mutant neurons *in vivo* and in the context of wild-type cells.

Most genetic approaches to mouse brain function have utilized either null mutations or targeted gene inactivation. The latter is most often achieved with "floxed" genes and their site-specific recombination by Cre recombinase expressed under control of neuron or glial-specific promoters. However, the activity of neuronal regulatory elements in Cre transgenic mice is often not restricted to specific neuronal subtypes, such as in Thy1.2-Cre, PrP-Cre, or NSE-Cre mice (Weber et al. 2001; Campsall et al. 2002; Kwon et al. 2006). Other Cre transgenes

express already in multipotent neural precursor cells, for example, in Nestin-Cre and Emx1-Cre mice (Tronche et al. 1999; Gorski et al. 2002) or include subcortical projection neurons, such as in CaMKII α mice (Minichiello et al. 2002). Recently, we generated transgenic mice for the selective gene targeting of hippocampal and neocortical pyramidal neurons, by placing Cre expression under control of the endogenous regulatory sequences of the *Nex1* (*Neurod6*) gene (Goebbels et al. 2006). NEX is a neuronal bHLH protein that is specific to newly generated glutamatergic pyramidal neurons of the cortex (Bartholoma and Nave 1994; Schwab et al. 1998) and dispensable for brain development in homozygous *Nex1* mouse mutants (Schwab et al. 1998, 2000).

A drawback of constitutive neuronal Cre expression is the recombination of a large number of densely packed cells, often preventing the analysis of gene functions at the single-cell level or at later stages of development. This limitation can be solved by inducible Cre recombination, experimentally controlled by administration of tamoxifen. Here, a modified version of Cre recombinase (termed CreERT2), resulting from the N-terminal fusion of Cre to a mutated human estrogen receptor (ER) ligand-binding domain, allows the temporal control of Cre-mediated recombination (Feil et al. 1997; Metzger and Chambon 2001). Peripheral administration of tamoxifen (a synthetic ER ligand) to mice induces the dissociation of the cytosolic fusion protein from HSP90, the nuclear import of CreERT2, and the site-specific recombination of loxP-flanked target genes. For some cell types in the nervous system, this approach has been successfully used to induce Cre-mediated genomic recombination, such as for neural progenitor cells (Burns et al. 2007), oligodendrocytes (Leone et al. 2003; Traka et al. 2010; Pohl et al. 2011), astrocytes (Hirrlinger et al. 2006), and serotonergic neurons of the brain stem (Mori et al. 2006; Weber et al. 2009). For a diverse group of neurons, placing CreERT2 expression under control of the cloned Thy1.2 promoter (Young et al. 2008) or the CamKII α promoter (Erdmann et al. 2007) resulted similarly in inducible Cre activity. However, the cell type specificity of these transgenes was not well defined, and reporter gene activation could be found throughout the CNS, including vital subcortical areas (Erdmann et al. 2007, 2008; Young et al. 2008).

Recent work in mouse mutants has established that oligodendrocytes support axonal integrity, independent of myelination itself (Griffiths et al. 1998; Lappe-Siefke et al. 2003; Yin et al. 2006). The molecular mechanisms of such support functions are not understood but may involve metabolic and anti-inflammatory processes (Nave 2010). Mice with a specific ablation of peroxisomal function in

oligodendrocytes develop progressive neurodegeneration with severe demyelination and axonal loss, whereas oligodendrocyte survival is not compromised. Moreover, peroxisome dysfunction leads to a massive reactive gliosis that precedes the infiltration of blood-derived B and T cells (Kassmann et al. 2007). Similarly, overexpression of proteolipid protein, the major CNS myelin protein, in transgenic mice causes invasion of inflammatory blood cells into the brain parenchyma (Ip et al. 2006). A common feature of these mouse lines are changes in lipid metabolism that might promote inflammation (Kassmann and Nave 2008). In contrast, physical ablation of oligodendrocytes by diphtheria toxin expression failed to trigger a similar T cell response (Traka et al. 2010; Pohl et al. 2011) suggesting that live oligodendrocytes are responsible for the signals that trigger inflammation.

Here, we report the inducible and cell type-specific targeting of cortical and hippocampal pyramidal neurons in *NEX-CreERT2* mice, generated as a knock-in of the *CreERT2* gene into the *Nex1* locus. We demonstrate the utility of *NEX-CreERT2* mice for multiphoton imaging of single neurons *in vivo* and for achieving the ablation of adult pyramidal neurons *in vivo* mice by inducing the expression of diphtheria toxin. Using this approach, we show that in contrast to dying oligodendrocytes, the ablation of pyramidal neurons recruits immune cells into cortical gray matter, which is of relevance for understanding neuroinflammatory processes in neurodegenerative diseases.

Materials and Methods

Gene-Targeting Vector

For assembly of the targeting vector (pAA-NEX-CreERT2), we used *Nex1* genomic DNA fragments from the vector pNEX-Cre (Goebbels et al. 2006) and *CreERT2* cDNA fragments from plasmid pCreERT2 (Feil et al. 1997). The “short arm” of the targeting vector represents a 1.47-kb fragment located immediately upstream of the *NEX* coding region: the 5' part of this fragment was cloned as a *KpnI/XbaI* fragment (824 bp) into pBluescript-KS (Stratagene) and the 3' part was generated by polymerase chain reaction (PCR) using primers KICreERNEX1-s: 5'-AGA CTT CCG TGG CTC TTA GAAC-3' and KICreERNEX2-as: 5'-CAT GGT TCT TTA ACC TTA ATT TAC-3' and pNEX-Cre as template DNA. The 5' part of the *CreERT2* coding sequence was generated by PCR (with pCreERT2 as template), using primers KICreERNEX3-s: 5'-ATT AAG GTT AAA GAA CCA TG TCC AAT TTA CTG ACC G -3' and KICreERNEX4-as: 5'-TTC GGA TCC GCC GCA TAA CCAG -3'. Subsequently, the 3' part of the short arm was fused to the 5' part of *CreERT2* by “gene SOEing” PCR (Horton 1995, 1997) with primers KICreERNEX1-s and KICreERNEX4-as and subcloned as an *XbaI/BamHI* fragment into the targeting vector. The *CreERT2* coding sequence was completed by subcloning a 1.8-kb *BamHI/SalI* fragment (containing an SV40 polyadenylation signal) from plasmid pCreERT2. Next, a neomycin resistance gene flanked by *FRT* sites from pFRTNeo was amplified by PCR with primers SpeINeo-s: 5'-CGC CGC CAC TAG TCT CGA GAC CGG T-3' and NdeINeo-as: 5'-GGG AAT TCC ATA TGG CGA TCG CGG CCG GCC AGA TCTC-3' and subcloned as a *NdeI/SpeI* fragment 3' to the *CreERT2* coding sequence. Finally, the 5.3 kb “long arm” harboring the 3' region of exon 2 and downstream sequences of the *Nex1* gene was subcloned as a *SpeI* fragment. The final targeting vector (pAA-NEX-CreERT2) was verified by restriction analysis, DNA sequencing, and FLP-mediated recombination of the neomycin resistance gene *in vitro*.

Gene Targeting in Embryonic Stem Cells, Transgenic, and Mutant Mice

Murine embryonic stem (ES) cells (SV129/OLA) were electroporated with the *SacII* linearized targeting vector pAA-NEX-CreERT2. A nested PCR screening strategy was used to identify ES cell clones harboring the

correct genomic targeting event. Four correctly targeted ES cell clones were used to generate chimeric mice by injection into C57Bl/6 derived blastocysts. Germ line transmission was verified by breeding chimeric founders to C57Bl/6 wild-type mice. Heterozygous offspring were crossed to FLP deleter mice (Rodriguez et al. 2000) on a C57Bl/6 background to remove the neomycin selection cassette. Genomic DNA from tail biopsies was prepared using Invisorb Spin tissue Mini Kit (Invitex) according to manufacturer's instructions. Routine genotyping was performed by PCR using primers Exon1-s, Nex-ORF-as, and Cre-as (5'-GAGTCTGGAATCAGTCTTTTC-3', 5'-AGAATGTGGAGTAGGGT-GAC-3', 5'-CCGCATAACCAGTGAAACAG-3'), respectively. Genotyping of Cre reporter lines R26R-lacZ (Soriano 1999), R26R-Yellow Fluorescent Protein (YFP) (Srinivas et al. 2001), R26R-td-tomato-mEGFP (mTmG) (Muzumdar et al. 2007), CAG-CAT-EGFP (Nakamura et al. 2006), and R26R-DTA (Brockschneider et al. 2004, 2006) has been described. Detailed genotyping PCR protocols are available upon request. All animal experiments were carried out in compliance with approved animal policies of the Max Planck Institute of Experimental Medicine.

Tamoxifen Injections

Tamoxifen solution (10 mg/mL) was freshly prepared by vigorous shaking of tamoxifen freebase (T5748-56, Sigma) in corn oil (C8267, Sigma) at room temperature (RT) for 45 min and stored at 4 °C. For “prenatal” induction, a single dose of 5 mg tamoxifen (500 μ L) was administered to pregnant females by injection (intraperitoneally [i.p.]) at E19. For “perinatal” induction, lactating dams were injected with tamoxifen at a dosage of 100 mg/kg body weight for 5 consecutive days starting at P1. Finally, for adult induction (≥ 3 weeks of age), tamoxifen was injected at a dosage of 100 mg/kg body weight for 2-10 consecutive days.

X-gal Histochemistry

Mice were anesthetized with avertin and perfused with 4% paraformaldehyde (PFA) in 0.1 M phosphate buffered saline (PBS). Brains were postfixed at 4 °C in 4% PFA for 1 h. Free-floating vibratome sections (40-50 μ m) were incubated at 37 °C in X-gal solution (5 mM $K_3[Fe(CN)_6]$, 5 mM $K_4[Fe(CN)_6]$, 2 mM $MgCl_2$, 1.2 mg/mL 5-bromo-2-chloro-3-indolyl-b-D-galactopyranoside in PBS) for 20 min to overnight in the dark, rinsed in PBS (2-3 times), and mounted in Eukitt. Digital images of stained sections were obtained using Axiophot microscope (Zeiss, Germany). All images were processed with Photoshop CS3 software (Adobe).

Histology and Immunostaining

Mice were anesthetized with avertin and perfused with 4% PFA in 0.1 M phosphate buffer. Brains and spinal cords and were postfixed in 4% PFA for 1 h to overnight at 4 °C. After postfixation, tissues were either embedded in paraplast or stored in 1% PFA in 0.1 M PBS at 4 °C until further processed. Free-floating vibratome sections (40-50 μ m) were incubated overnight with primary antibodies against Calbindin (mM; 1:300, Sigma), Calretinin (pRb; 1:1000, Chemicon), GAD67 (mM; 1:1000, Chemicon), GFAP (mM; 1:200, Novocastra), GFP (pGoat; 1:1000, Rockland), GFP (pRb; 1:1000, Abcam), NeuN (mM; 1:100, Chemicon), Olig2 (pRb; 1:20,000, a gift of C. Stiles), and Parvalbumin (pRb; 1:200, Swant).

Sections were further incubated with corresponding secondary antibodies raised in either goat or donkey, Cy2 (1:10 000, Jackson ImmunoResearch), Cy3 (1:10 000, Jackson ImmunoResearch), and Alexa-488 and Alexa 555 (1:2000, Invitrogen) for 1 h at RT. For the analysis of neurodegenerative changes, 5-7 μ m thick paraplast embedded brains sections were used. Tissue sections were stained either with histological stains such as hematoxylin-eosin (H&E, Merck); cresyl violet (Nissl); and Fluoro-JadeC (Fluoro-JadeC [FJC], Histo-Chem Inc.), according to manufacturer's instructions or incubated with primary antibodies against FNP7 (mM; 1:150, Zytomed Systems), GFAP (pRb; 1:200, DAKO), Iba1 (pRb; 1:1000, Wako), MAP2 (mM; 1:1000, Sigma), CD3 (T cell receptor, 1:150, Serotec), and CD45R (1:100, Santa Cruz) for DAB-based immunostaining (Dako-LSAB₂ kit was used according to manufacturer's

instructions). Digital images of stained sections were obtained using Zeiss 510-meta LSM (Zeiss), Axiophot (Zeiss), DMRXA (Leica, Germany) microscopes. All images were processed with Photoshop CS3, Illustrator CS3 software (Adobe), ImageJ (NIH, Bethesda, USA; <http://rsbweb.nih.gov/ij>) and Fiji (Image processing package based on ImageJ).

Confocal Imaging of Neuronal Morphology

Two- to three-month-old mice were perfused intracardially with freshly prepared 4% PFA in 0.1 mM phosphate buffer. After perfusion brains were postfixed in 4% PFA for 1–2 h at 4 °C. Coronal brain sections (vibratome, 50–100 μ m thick) were immunostained overnight at 4 °C with primary antibodies against GFP [either (pGoat; 1:1000, Rockland) or (pRb; 1:1000, Abcam)]. Alexa-488-coupled anti-goat/rabbit secondary antibody (Invitrogen) was used for 2 h at RT for detecting corresponding primary antibodies. After rinsing 3 times in 0.1 mM PBS at 4 °C, sections were mounted on superfrost glass slides using Aqua Polymount. A Zeiss laser scanning confocal microscope (Zeiss, 510 Meta) was used to acquire z-stacks of YFP-positive neurons at optical

slices of 0.53 μ m with a 63 \times objective (1.4 numerical aperture). All images were processed with ImageJ (NIH; <http://rsbweb.nih.gov/ij>) and Fiji (Image processing package based on ImageJ). For 3D visualization of confocal z-stacks as volumes, Java-based “ImageJ 3D Viewer” plugin developed by Benjamin Schmid (Biozentrum, Würzburg, Germany) was used.

Two-Photon Laser Scanning Microscopy (2P-LSM) and Image Processing

Imaging was carried out with transgenic mice at 6–8 weeks of age under general anesthesia using a gas mixture of O₂:N₂O (1:1) loaded with 5% isoflurane in a closed box (flow rate: 1000 mL/min). After initial sedation, anesthesia was maintained by a mask on a heated plate and reduced flow rate (N₂O: 100–200 mL/min; O₂: 200–300 mL/min; 1.5–2% isoflurane). The respiration rate was kept below 2 per second by adjusting the isoflurane dosage. The skull was attached to a custom-made ring by cement to reduce respiratory-induced movements. A cranial window through the parietal bone was produced inside the

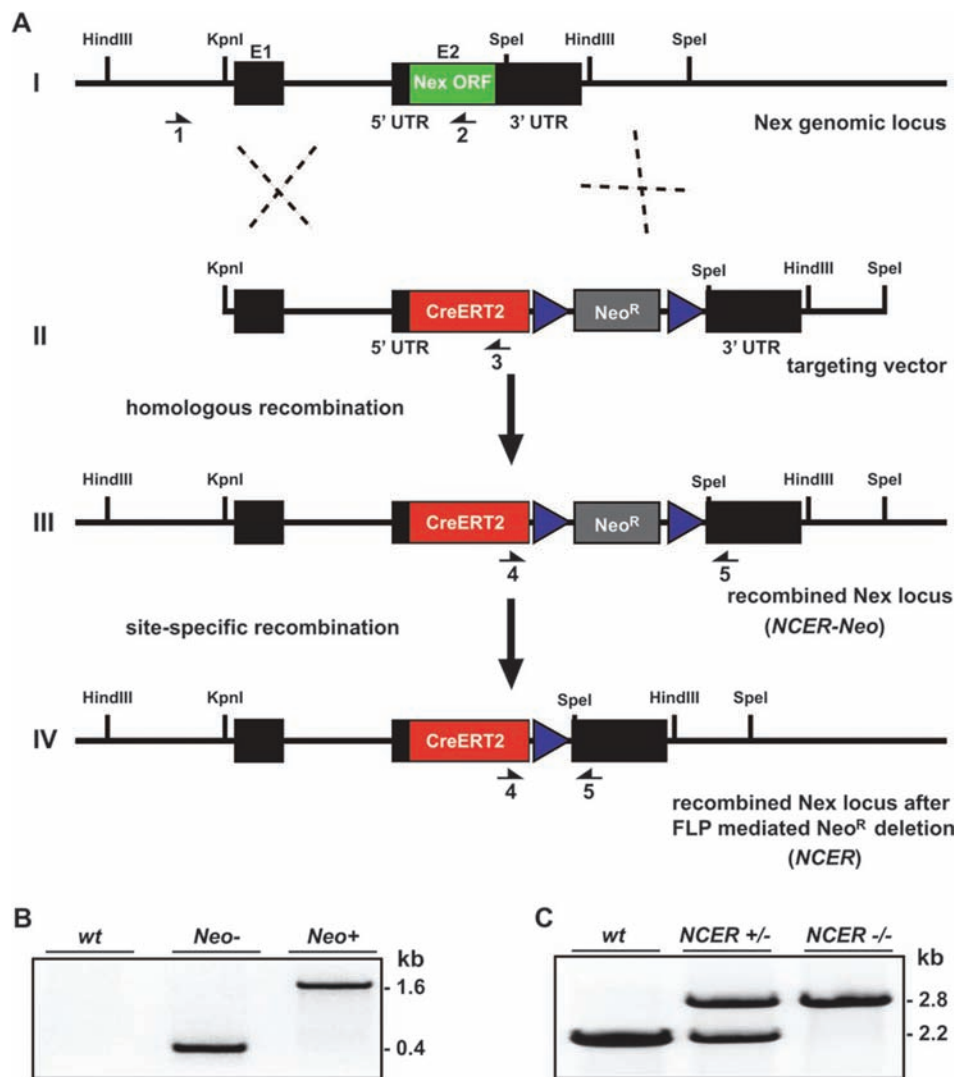


Figure 1. Strategy to “knock-in” *CreERT2* into the mouse *Nex1* gene. (A) 1) Genomic structure of the wild-type *Nex1* allele. The locus comprises 2 exons (E1, E2; black boxes). The entire coding region (ORF; green box) is located on exon 2. 2) *NEX-CreERT2* targeting vector. The construct harbors 5' and 3' homology arms (black), the *CreERT2* cDNA (red box) fused to the start codon of the *Nex1* gene and a neomycin resistance cassette (Neo^R; gray box) flanked by 2 FRT sites (blue triangles). 3) *NEX-CreERT2* allele (*NCEr-Neo*) after homologous recombination in murine ES cells. 4) *NEX-CreERT2* allele after site-specific removal of the Neo^R cassette (*NCEr*) by breeding *NCEr-Neo* mice to FLP deleter mice. Arrows #1–5 indicate primer locations for PCR-based characterization of *NCEr-Neo* and *NCEr* mice. (B) FLP-mediated removal of the Neo^R cassette is verified by PCR with primers #4, 5 on genomic tail DNA from wt (no amplification), heterozygous *NCEr* mice before (Neo⁺; 1.6 kb), and after breeding to FLP deleter mice (Neo⁻; 400 bp). (C) PCR with primers #1–3 on genomic tail DNA from wild type (wt; 2.2 kb), *NCEr* heterozygous (*NCEr*^{+/-}; 2.2 and 2.8 kb), and *NCEr* homozygous mice (*NCEr*^{-/-}; 2.8 kb) confirms correct targeting of *CreERT2* cDNA into the *Nex1* locus. Note: primer #1 is located outside the targeting vector.

ring close to the sagittal suture. The exposed cortex was covered by a glass coverslip. Body temperature was kept constant (36–38 °C) throughout the experiment.

In vivo imaging was performed by a custom-made 2P-LSM equipped with an fs-pulsed titanium-sapphire laser (Chameleon Ultra II, Coherent, Glasgow, UK) and a long-distance 20×/1.0 NA water immersion objective (Zeiss, Jena, Germany). For excitation, the laser was set at 925 ± 5 nm. The fluorescence signal of Enhanced Green Fluorescent Protein (EGFP)-positive pyramidal neurons was collected by a photomultiplier tube (Hamamatsu, Japan) through a 510 ± 42 nm band-pass filter (Semrock). Uniformly spaced (0.8–2 μm) planes of 125 × 125 to 500 × 500 μm² regions of the cerebral cortex were recorded and processed to obtain z-stacks of images (512 × 512 or 1024 × 1024 pixels in size). Image processing was performed using Matlab (version 7, MathWorks, Ismaning, Germany) and ImageJ (NIH; <http://rsbweb.nih.gov/ij>). Three-dimensional visualization was performed as described before. For 3D visualization of image stacks as volumes, Java-based ImageJ 3D Viewer plugin developed by Benjamin Schmid (Biozentrum) was used.

Results

To achieve *CreERT2* expression under control of regulatory sequences from the endogenous *Nex1* gene, we employed a “knock-in” strategy based on homologous recombination in mouse ES cells (Fig. 1). Using a targeting vector, in which the NEX coding region in exon 2 was replaced by a CreERT2 expression cassette, we generated the mouse mutant *NEX-CreERT2-Neo* that harbors the CreERT2 cassette adjacent to a neomycin resistance (*Neo^R*) gene driven by a thymidine kinase promoter (placed in antisense orientation), as shown in Figure 1A. Subsequently, we removed the *Neo^R* gene *in vivo* by breeding to FLP deleter mice (Rodriguez et al. 2000) and FLP-mediated site-specific recombination (Fig. 1A). The resulting mutant allele (in *NEX-CreERT2* mice) carries a residual FLP site 3' to the CreERT2 cassette, thus providing a nearly “wild-type” genomic environment with respect to *Nex1* gene expression. Correct genomic targeting and removal of *Neo^R* was verified by a PCR-based analysis of genomic DNA (Fig. 1B,C and data not shown).

Cre-Mediated Recombination in Mature Pyramidal Neurons

For a detailed functional analysis of CreERT2 expression, heterozygous mutants from mouse lines *NEX-CreERT2* (in subsequent text and figures referred to as *NCER-Neo*) and *NEX-CreERT2 (NCER)* were crossbred with several transgenic reporter lines that conditionally express β-galactosidase (Soriano 1999), YFP (Srinivas et al. 2001), membrane-tagged EGFP (Muzumdar et al. 2007), and cytoplasmic EGFP (Nakamura et al. 2006), following Cre-mediated deletion of

a floxed “stop-cassette.” At the age of 3–4 weeks, double transgenic mice were injected i.p. with tamoxifen (100 mg/kg), a treatment repeated daily for 10 consecutive days and analyzed between 1 and 2 months after the last injection.

Overall, the recombination detected in young adult mice was in the same subset of brain areas that we previously described in *NEX-Cre* mice (Goebbels et al. 2006 and Table 1). By X-gal histochemistry, serial coronal brain sections from *NCER* mice with a LacZ reporter (a genotype termed *NCER^RR26R-floxLacZ* in the following) revealed prominent staining of the pyramidal layer in the hippocampal CA1–3 region (Fig. 2C,D,H). Also the majority of mossy cells in the hilar region (CA4) were labeled, but no granule cells in the dentate gyrus (Fig. 2H). In the neocortex, Cre-mediated recombination appeared restricted to only a subset of pyramidal neurons, homogeneously distributed (Fig. 2A,B,G and Supplementary Fig. 1). When compared with the neocortex, a modest increase in Cre recombination was observed in the cingulate cortex, as well as the retrosplenial granular and agranular cortices (Fig. 2A,B,C; Supplementary Fig. 1), which extend efferents into the anterior thalamic nuclei, the lateral dorsal thalamic nucleus, and the hippocampal anlage. This recombination pattern confirms a sparse NEX mRNA expression in the adult mouse brain (Schwab et al. 1998; see also Allen brain atlas, Supplementary Fig. 2; Table 1).

Cre recombination under control of the NEX promoter will permanently mark transient NEX expression domains, such that in conventional *NEX-Cre* mice (Goebbels et al. 2006), the adult pattern of reporter gene expression most likely represents both transient and permanent NEX expression domains. Applying a late recombination protocol (starting 3–4 weeks after birth) to *NCER* mice, we identified transient NEX promoter activity in neurons of the dentate gyrus, olfactory bulb, thalamus, brain stem, and spinal cord (Fig. 2; Supplementary Fig. 1; and Table 1). In line with barely detectable expression of NEX mRNA outside of neocortex and hippocampus (e.g., in the cerebellum) (Schwab et al. 2000), cerebellar granule cell labeling was minimal (Fig. 2E; Supplementary Fig. 1H; and Table 1). We also could not detect recombined neurons in the absence of tamoxifen, thus demonstrating that cytoplasmic CreERT2 retention is tight (data not shown). Virtually identical results were obtained when we analyzed mice from line *NCER-Neo* (Supplementary Fig. 3A) that still harbor the neomycin resistance cassette (in antisense orientation) within the targeted *Nex1* gene.

To further evaluate the identity of Cre recombinant cortical cells in *NCER* mice, we utilized a second line of YFP reporter mice (Srinivas et al. 2001) and induced CreERT2 activity by

Table 1

Domains of Cre-mediated recombination in *NEX-CreERT2/+*R26R-LacZ* mice (age 3 months) after tamoxifen induction at 4 weeks of age

Modest/complete recombination	Scattered recombination (salt and pepper)	No recombination ^a
Hippocampus, CA1–3	Anterior olfactory nucleus	Main olfactory bulb
Cingulate cortex	Neocortex: layers II–VI	Thalamus
Retrosplenial agranular cortex	Dentate gyrus (hilar cells in polymorphic layer)	Dentate granule cells ^b
Retrosplenial granular cortex	Subiculum (including presubiculum and parasubiculum)	Hypothalamus
Induseum griseum	Tenia tecta	Midbrain
	Clastrum	Hindbrain
	Piriform cortex	Medulla oblongata
	Entorhinal cortex	Pons
	Amygdala	Dorsal horn of spinal cord
	Cerebellar granular cells	

^aUp to 10 recombined cells per brain slice in these structures.

^bPerinatal tamoxifen treatment leads to scattered recombination in dentate granule cells.

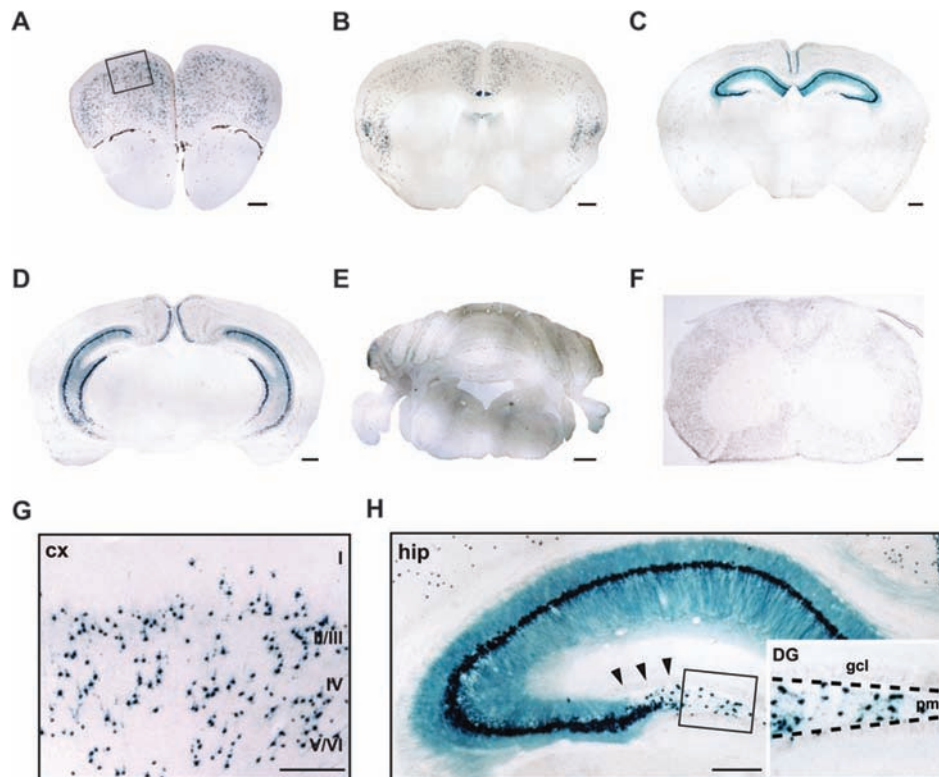


Figure 2. Inducible CreERT2-mediated recombination in adult brains of *NCER* mice. *NCER**R26R-floxLacZ** double transgenic mice at 3–4 weeks of age were injected with tamoxifen (100 mg/kg body weight) for 10 consecutive days. CreERT2-mediated recombination was analyzed by X-gal histochemistry on coronal vibratome sections (40 μ m) at 2–3 months of age. (A–F) Overviews reveal β -galactosidase expression in neocortex, induseum griseum, and hippocampus, whereas only few cerebellar granular cells and no spinal cord neurons were recombined. (G) Blow up of boxed area in A. Scattered recombination in layers II–VI of motor cortex. (H) Virtually all pyramidal cells of the hippocampal CA1–3 region express β -galactosidase. While recombination is completely absent from dentate granule cells (arrows), a subset of cells in the dentate hilar region, most likely mossy cells, express β -galactosidase (inset). Abbreviations: cx, neocortex; DG, dentate gyrus; gcl, granule cell layer; hip, hippocampus; pml, polymorphic layer; I–VI, cortical layers. Scale bars: 500 μ m (A–E); 250 μ m (F–H).

injecting tamoxifen for 10 days in 4- to 5-week-old mice (as described above). We then used immunolabeling at the age of 3–4 months and combined a fluorescent reporter (YFP) of Cre activity with various cell type-specific neural markers. When analyzed by confocal microscopy, all recombinant cells could be identified as large NeuN-positive projection neurons (Fig. 3A–C; Supplementary Fig. 4A–C). Neither interneurons nor astrocytes or oligodendrocytes were recombined in *NCER**R26R-floxYFP** mice, when using calbindin, calretinin, parvalbumin, GAD67, GFAP, and Olig2 as respective cell type-specific markers (Fig. 3D–F and Supplementary Fig. 4D–F), confirming that in the forebrain Cre recombination is restricted to pyramidal neurons.

Tamoxifen Dosage-Dependent Gene Recombination

We next explored various protocols of tamoxifen administration at distinct developmental and adult stages. First, we determined the impact of treatment duration (from 1 to 8 consecutive daily i.p. injections, starting at 3–4 weeks of age) on the number of recombined cells in the hippocampus (Fig. 4A,B) and neocortex (Supplementary Fig. 5). While a single tamoxifen injection was ineffective in inducing recombination anywhere in the brain (data not shown), the number of recombined cells gradually increased from 2 to 8 days of treatment, both in hippocampus (Fig. 4A,B) and in neocortex (Supplementary Fig. 5). Importantly, treatment between 2 and 5 days produced a quantity of recombined hippocampal

neurons that is suitable for single-cell analysis (Fig. 4A). Tamoxifen treatment in 5- to 6-month-old mice produced similar results (data not shown).

Tamoxifen administration at prenatal stages can induce developmental defects and premature abortion (Jordan and Murphy 1990; Danielian et al. 1998). Therefore, we tested the efficacy of 2 “mild” application protocols, either a single tamoxifen injection (5 mg) to the female at E19 during late pregnancy (prenatal) or daily i.p. injections (100 mg/kg body weight) to the female for 5 consecutive days starting immediately after delivery (“postnatal”), such that pups receive tamoxifen through the milk. Immunostaining for YFP at postnatal day (P) 28 revealed that both administration paradigms produced significant quantities of recombined cells in neocortex (Fig. 4E,F) and the hippocampal CA1–3 region (Supplementary Fig. 6A) of *NCER**R26R-floxYFP** mice. Both paradigms also induced recombination in dentate granule cells (Fig. 4C,D) providing further evidence that CreERT2 expression faithfully recapitulates transient NEX promoter activity in dentate granule cells. As expected, the postnatal administration protocol produced more recombined cells in dentate gyrus (Fig. 4D) and cortex (Fig. 4F) when compared with the prenatal paradigm. Longer duration of tamoxifen treatment in the postnatal protocol is also reflected by the broader radial distribution of recombined granular cells that settle in the granule cell layer according an inside-in order (Fig. 4C). As for adult treatment, recombination induced by perinatal tamoxifen

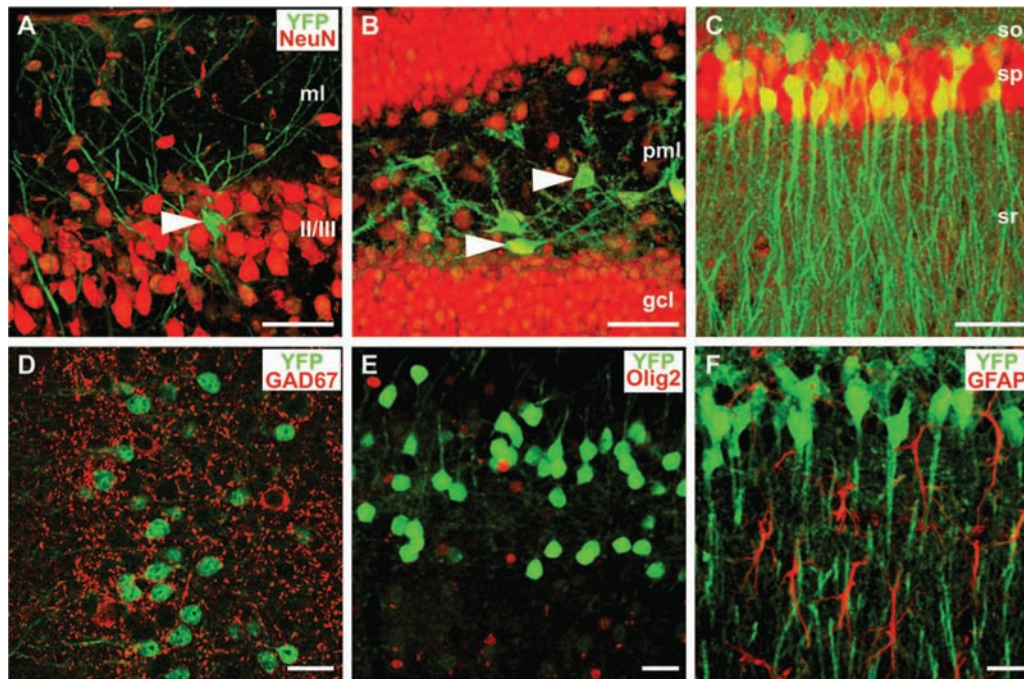


Figure 3. Nex promoter activity in neocortex is restricted to principal neurons. Confocal images of fluorescent immunostainings for a CreERT2-induced YFP reporter and the pan-neuronal marker NeuN (A–C) or neural cell type-specific markers (D–F) on coronal vibratome sections (40 μ m) from 2- to 3-month-old *NCER^{*}R26R-floxYFP* mice after tamoxifen injections for 10 consecutive days starting at 3–4 weeks of age. (A) Individual YFP-positive neuron (arrowhead) in layers II/III of motor cortex. (B) Mossy cells in the polymorphic layer (pml) of the hilar region express YFP (arrowheads), whereas dentate granule cells (gcl) completely lack NEX promoter activity at this age. (C) In CA1, NeuN-positive cells in the pyramidal cell layer (sp) coexpress YFP, the remaining NeuN-positive cells are mainly interneurons. (D–F) NEX promoter activity is completely absent from interneurons and glial cells as demonstrated by immunostaining for YFP and antibodies directed against pan-interneuronal marker GAD67 (D), Olig2 (oligodendrocytes; E) and GFAP (astrocytes, F). All images are 3D volume rendered from confocal z-stacks and pseudocolored using ImageJ. Abbreviations: gcl, granule cell layer; ml, molecular layer; pml, polymorphic layer; so, stratum oriens; sp, stratum pyramidale; sr, stratum radiatum; II/III, cortical layers. Scale bars: 50 μ m (A–C); 20 μ m (D–F).

administration was completely absent from interneurons (Supplementary Fig. 6B,C) and glia cells (data not shown). In general, we did not observe toxic effects of tamoxifen on the pregnant (late stage) as well as lactating dams. However, perinatal tamoxifen treatment caused a marked reduction in body size (30–50%) of the offspring at 4 weeks of age. These mice displayed improper gait, most likely as a result of ongoing muscle degeneration in their hind limbs.

Single-Cell Imaging in Live Mice

NCER mice exhibit scattered recombination in a subset of cortical projection neurons. To further evaluate these mice as a suitable tool for “single-cell genetics,” we bred *NCER* mice to a reporter mouse line that conditionally expresses a cytoplasmic variant of EGFP (Nakamura et al. 2006). At 3–4 weeks of age, *NCER^{*}CAG-CAT-EGFP* mice were injected with tamoxifen for 2 or 10 consecutive days, and brains were analyzed 3–4 weeks later by confocal microscopy. The 3D volumes of EGFP-positive cells in different brain regions were calculated from confocal z-stacks acquired from sections of 50–100 μ m thickness (Fig. 5). Analysis of mice that were tamoxifen injected for only 2 days revealed a Golgi-like staining of pyramidal neurons that allowed the tracing of single dendrites and axons in layers II/III and V of the neocortex and in the CA1 region of the hippocampus (Fig. 5A–C; Supplementary Video 1–3). In mice induced for 10 days, we were able to reconstitute the complete arborization of neurons in the indusium griseum (Fig. 5D) and cerebellar granule cells (Fig. 5E). As recombination was completely absent from the spinal cord, single motor axons of the cortical spinal tract could be imaged at

the thoracic level (Fig. 5F; Supplementary Video 4). Similarly, in the absence of recombination in dentate granule cells, we were able to image terminals of the perforant path that innervates the granule cell layer (Fig. 5G,H). Finally, by breeding *NCER^{*}R26R-floxYFP* mice to *GFAP-CreERT2* mice, which express CreERT2 in cortical astrocytes (Hirrlinger et al. 2006), we demonstrate the feasibility of this approach to image interactions between different cortical cell types (Supplementary Fig. 7).

The fluorescent labeling of single neurons in a “Golgi-like” fashion also permits the imaging of neuronal dynamics in living mice (Kasthuri and Lichtman 2007). As proof of principle for such a single-cell genetics approach, we imaged the arborization of individual pyramidal cells in the cortex of *NCER^{*}CAG-CAT-EGFP* mice by *in vivo* multiphoton imaging (Fig. 6A,B). After 2-day induction, we captured the complete arborization of individual pyramidal neurons in layers II/III of the motor cortex (Fig. 6A). Tamoxifen administration for 10 days allowed *in vivo* imaging of pyramidal neurons along the entire width of the motor cortex (Fig. 6B; Supplementary Video 5).

Noninvasive Ablation of Pyramidal Neurons Triggers T Cell Infiltration

Most animal models of neurodegeneration rely on invasive interventions, are prone to inflammatory side effects, and do not allow targeting of specific neural cell types. We therefore took advantage of *NCER* mice to specifically ablate pyramidal neurons in the adult brain by breeding to a mouse line that conditionally expresses the diphtheria toxin-A (DT-A)

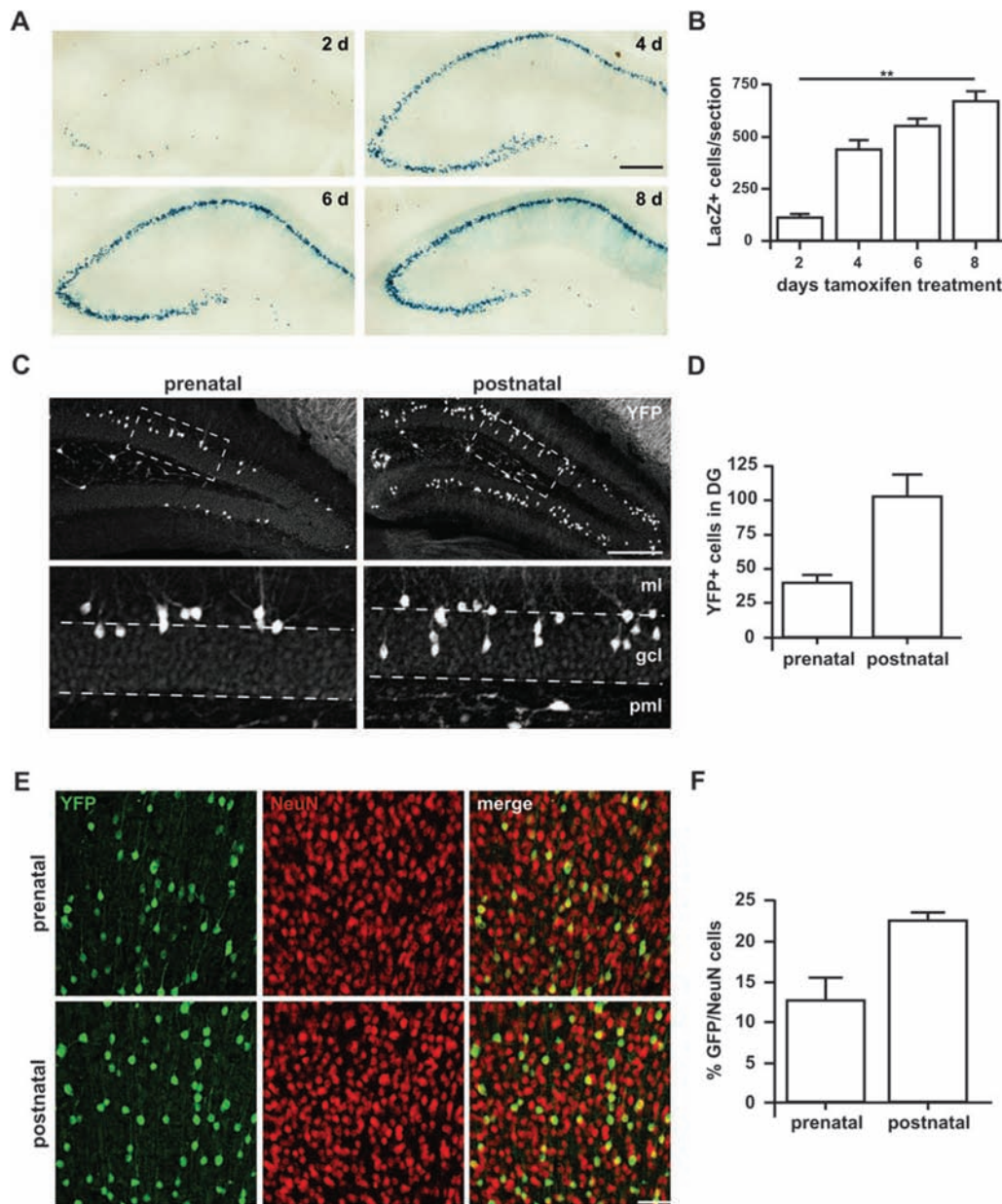


Figure 4. Tamoxifen induces dosage- and stage-dependent recombination in *NCER* mice. (A–B) *NCER-Neo**R26R-floxLacZ** mice exhibit tamoxifen dosage-dependent recombination in hippocampal CA1–3 subfields. CreERT2-mediated recombination was induced in *NCER-Neo**R26R-floxLacZ** mice by tamoxifen injection for 2–8 consecutive days beginning at 4–8 weeks of age. (A) Coronal vibratome sections (40 μ m) were analyzed by X-Gal histochemistry at 4–5 months of age. (B) Quantification of β -galactosidase-positive cells reveals a significant increase in the number of recombined pyramidal cells after 8 days tamoxifen treatment compared with a 2-day treatment ($n = 3$; $P = 0.006$, one-way analysis of variance; Kruskal–Wallis test). (C–F) Perinatal induction of CreERT2 activity results in recombination of dentate granule cells and projection neurons in hippocampus and neocortex. Tamoxifen was administered either by injecting pregnant females at E19 (one injection of 5 mg; “prenatal”) or by injecting lactating females for 5 consecutive days (100 mg/kg) starting on the day of parturition (“postnatal”). *NCER**R26R-floxYFP** mice were analyzed at 1 month of age by immunostaining for YFP on coronal vibratome sections (40 μ m). (C) YFP-positive granule cells are preferentially located in the outer shell of the granule cell layer (gcl) in mice that received prenatal tamoxifen treatment (blow up of boxed area in upper panel). In the postnatal paradigm, granule cells are more scattered within the granule cell layer, according to an “inside-in” pattern of migration. (D) Quantification of recombined granule cells following prenatal and postnatal tamoxifen treatment, respectively. Postnatal treatment produced more recombined granule cells, but this was not statistically significant. (E) Fluorescent micrographs of coronal brain sections from *NCER**R26R-floxYFP** mice double labeled for YFP and NeuN show scattered recombination in the motor cortex after prenatal and postnatal tamoxifen treatment. (F) Quantification of YFP- and NeuN-positive cells following prenatal and postnatal treatment. Abbreviations: gcl, granule cell layer; ml, molecular layer; pml, polymorphic layer. Scale bars: 300 μ m (A); 200 μ m (C), boxed: 50 μ m; 50 μ m (E).

fragment (Brockschneider et al. 2004, 2006). After 10 days of tamoxifen treatment, starting at 3 weeks of age, *NCER/+**R26R-floxDT-A** mice and *NCER/+* controls were sacrificed at 6 weeks of age. Staining with FJC, which selectively labels degenerating neurons, identified widespread neuronal death in the hippocampus of *NCER/+**R26R-floxDT-A** mice (Fig. 7A). Also the accumulation of MAP2 in neuronal cell bodies

indicated loss of cell integrity and marked apoptotic CA1 pyramidal neurons (Fig. 7A). Indeed, staining for the pan-neuronal nuclear marker NeuN revealed a 50% loss of NeuN-positive cells in the pyramidal cell layer of CA1 (Fig. 7A,B). We conclude that *NCER* mice are suitable to produce noninvasive, timely controlled lesions restricted to hippocampal (and few neocortical) pyramidal neurons in viable mice.

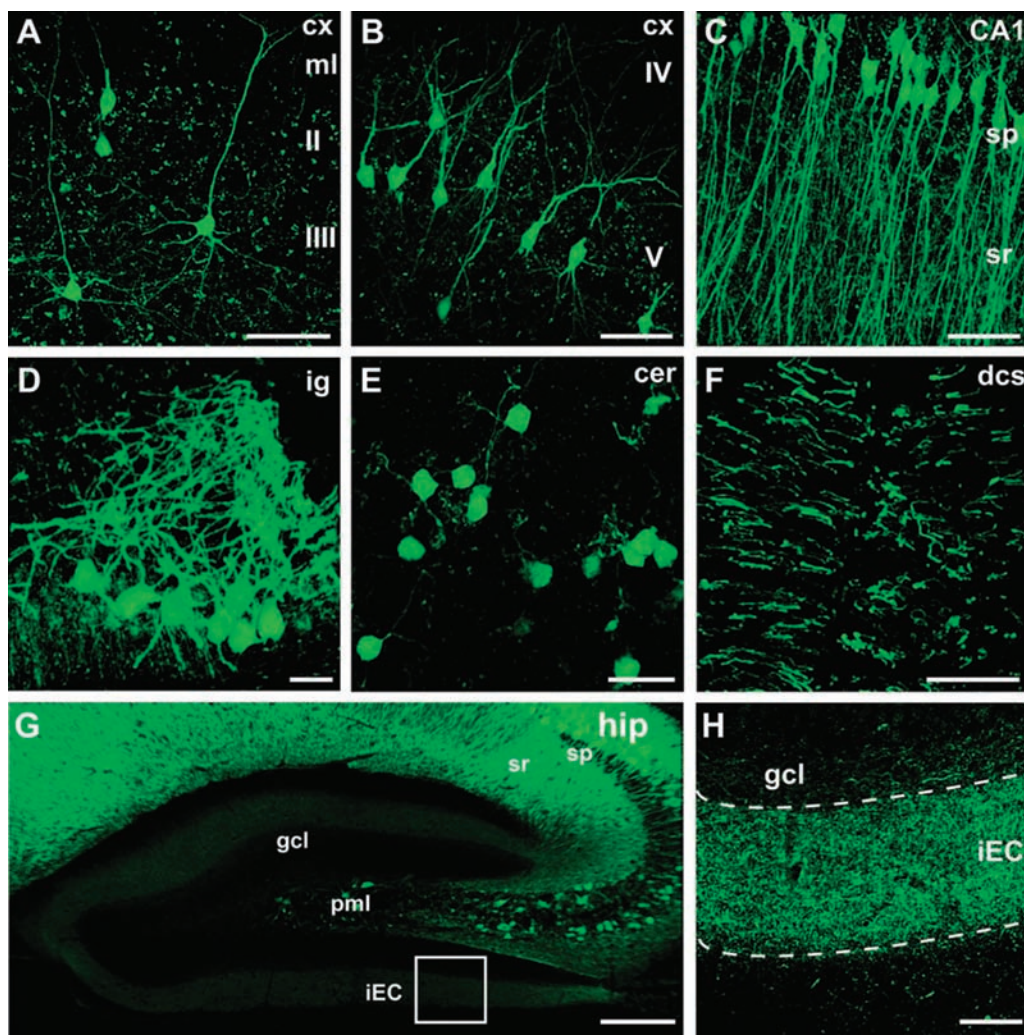


Figure 5. Analysis of pyramidal cell arborization by single-cell imaging in *NCER* mice. Confocal imaging of coronal vibratome sections (100 μ m) from *NCER***CAG-CAT-EGFP* mice at 7 months of age after tamoxifen injection for 2 days (A–C) and 10 days (D–H) starting at 4 weeks of age. Tamoxifen induction for 2 days allows visualization of individual EGFP-positive pyramidal cell arbors in cortical layers II/III (A), layer V (B), and the hippocampal CA1 subfield (C). Following 10 days of tamoxifen administration, imaging reveals a dense dendritic network of neurons in indusium griseum (D), whereas only a small number of cerebellar granule cells are recombined (E). *NCER***CAG-CAT-EGFP* mice also permit imaging of individual motor axons in the dorsal spinal cord (F). Sustained NEX promoter activity in entorhinal cortex (but not dentate granule cells) allows selective labeling of perforant path terminals on granule cells in the entorhinal cortex (G,H). (H) Blow up of boxed area in (G). All images are 3D volume rendered from confocal z-stacks and pseudocolored using ImageJ. Abbreviations: CA1, CA1 subfield of hippocampus; cer, cerebellum; cx, neocortex; dcs, dorsal column of spinal cord; gcl, granular cell layer; hip, hippocampus; iEC, projections from internal principal stratum of entorhinal cortex; ig, indusium griseum; ml, molecular layer; pml, polymorphic layer; so, stratum oriens; sp, stratum pyramidale; sr, stratum radiatum; II/III, cortical layers. Scale bars: 50 μ m (A–C,F,H); 20 μ m (D,E); 200 μ m (G).

Understanding the relationship between neural cell death and secondary immune responses is important for the etiology of autoimmune diseases of the CNS, such as multiple sclerosis. For example, neuroinflammation (including T cell invasion) is seen in mice with oligodendrocyte-specific mutations, which result in demyelination and degeneration of myelinated axons but not in oligodendroglial cell death (Ip et al. 2006; Kassmann et al. 2007). In stark contrast, DT-A mediated killing of oligodendrocytes does not trigger any T cell infiltration (Traka et al. 2010; Pohl et al. 2011; A Waisman, B Becher, personal communication). In this context, it is remarkable that after killing hippocampal neurons, we found, in addition to activated microglia/macrophages and reactive astrocytes (Fig. 8A), the infiltration of CD45R-positive B cells (Fig. 8B, top) and a massive invasion of CD3-positive T cells (Fig. 8B, bottom) in hippocampal gray matter. When quantified, the number of CD3-

positive T cells was significantly increased in the hippocampus of tamoxifen-treated *NCER/+ R26R-floxDT-A* mice compared with *NCER/+* controls (*NCER/+ R26R-floxDT-A* mice: 62 ± 18.2 cells per section [mean \pm standard deviation; $n = 3$ mice per group] vs. 0.67 ± 1.15 in controls). In contrast to hippocampal gray matter, we have not detected signs of gliosis or significant numbers of B or T cells in hippocampal fimbriae, that is, myelinated axons derived from degenerating hippocampal neurons (Fig. 8C and data not shown).

Consistent with the low number of recombined cells in the neocortex, neuronal degeneration and signs of inflammation were only marginally increased in *NCER/+ R26R-floxDT-A* mice (data not shown). However, in the cingulate cortex, where recombination frequency was slightly higher than in the neocortex, we observed activated microglia (Fig. 9A), astrogliosis (Fig. 9B), and a mild but significant infiltration of T cells

(Fig. 9C). We conclude that a minimal number of degenerating neurons are required to induce T cell invasion into gray matter areas. Whether these cells also contribute to the overall pattern of neurodegeneration awaits the generation of T cell-deficient double mutant mice.

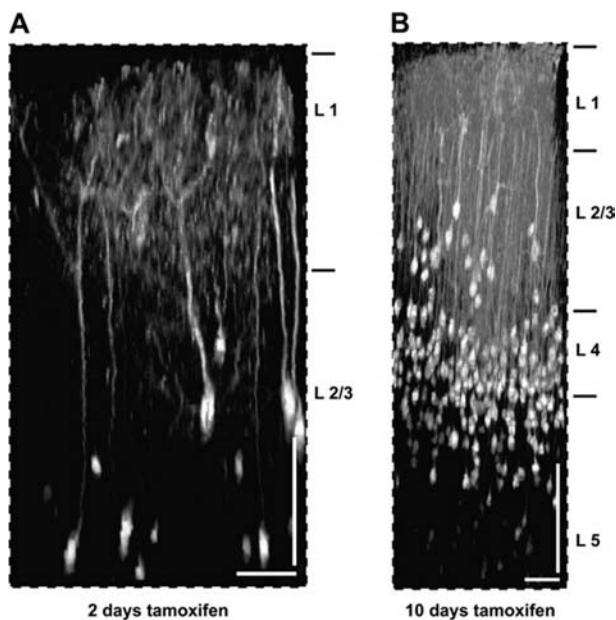


Figure 6. *In vivo* 2-photon imaging of individual pyramidal neurons in NCER mice. 2-photon imaging of neocortical projection neurons was carried out through a cranial window in the motor cortex sealed with a cover glass. Fluorescent image stacks were recorded in *NCER***CAG-CAT-EGFP* mice at 7–8 weeks of age following tamoxifen induction (100 mg/kg body weight) for 2 (A) and 10 days (B) starting at 3 weeks of age. Data were acquired with a pumped titanium:sapphire oscillator using a 20 \times water immersion lens with NA 1.0 (Zeiss). Note different scales of imaging depth in A and B. Tamoxifen induction for 10 days permits imaging of projection neurons throughout the entire depth of the neocortex (~800 μ m). Dimensions of cortical layers (L) are indicated. Images are presented as a 3D volume rendered from fluorescent image stacks. Scale bars: A,B: 50 μ m (horizontal); 100 μ m (vertical).

Discussion

We have described a novel knock-in mouse line that expresses CreERT2 under control of regulatory sequences of the *Nex1* gene. Due to the very restricted expression pattern, *NEX-CreERT2* mice allow inducible, highly selective genetic manipulations of neocortical and hippocampal projection neurons in the adult brain of viable mice.

Cre-Mediated Recombination in Mature Pyramidal Neurons

Tamoxifen-induced reporter expression in the adult brain of *NEX-CreERT2* mice revealed expression of the *Nex1* locus in a subset of brain areas that we previously defined in conventional *NEX-Cre* mice (Goebbels et al. 2006). The adult pattern of *Nex1* promoter activity faithfully reproduces NEX mRNA expression (Schwab et al. 1998; see also Allan brain atlas at <http://www.brain-map.org>). Importantly, CreERT2-mediated recombination is completely absent from interneurons, oligodendrocytes, and astrocytes as well as non-neural cells. Adult tamoxifen administration also allowed us to distinguish brain regions with sustained NEX expression from those with transient NEX promoter activity, such as spinal cord and deep cerebellar nuclei. We also confirm a transient NEX expression in dentate granule cells (Schwab et al. 2000; Goebbels et al. 2006) that ceases by 3 weeks of age. Transient promoter activity indicates a role for NEX during the initial differentiation of these brain regions but not for their maintenance in the mature brain. Areas with sustained *Nex1* promoter activity include the hippocampal CA1–3 region and dentate hilus, induseum griseum, and the cingulate cortex (reviewed in Table 1). While virtually all projection neurons express NEX during cortical development (Goebbels et al. 2006), only a small subset of projection neurons in cortical layers II–V maintain *Nex1* promoter activity in the adult brain.

NEX null mutants display impaired spatial learning (O Ucar and M.H.S., in preparation) and NEX cooperates with NeuroD2, a closely related neuronal bHLH protein (Kume et al. 1996; Yasunami et al. 1996), to promote long-range axogenesis

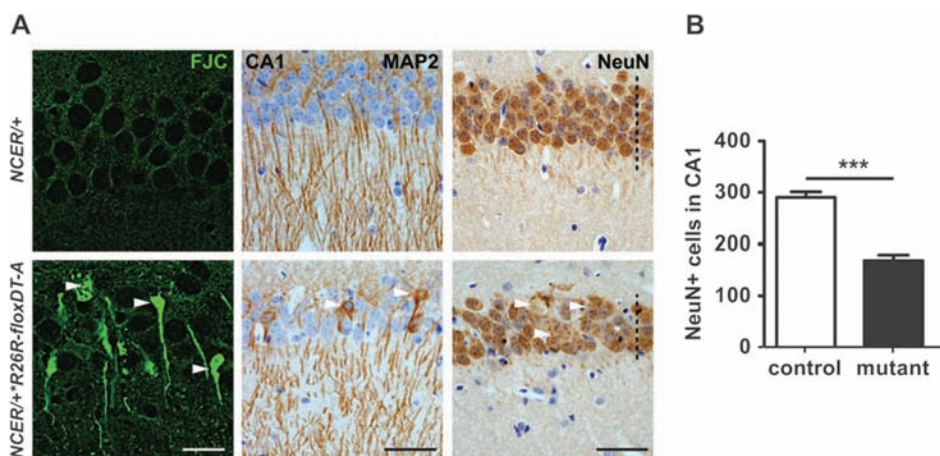


Figure 7. Selective ablation of adult hippocampal pyramidal neurons by NCER-mediated diptheria toxin expression. (A) Expression of DT-A in *NCER**/**R26R-floxDT-A* mice causes widespread death of hippocampal pyramidal neurons (arrowheads) as demonstrated by FJC staining (left panels). Accumulation of the dendritic marker Map2 in neuronal cell bodies (arrowheads; middle panels) supports neuronal degeneration. Immunostaining for NeuN reveals thinning of the pyramidal cell layer and loss of pyramidal cell somata in *NCER**/**R26R-floxDT-A* mice (right panels). Heterozygous NCER controls (*NCER**/*+*) and mice additionally harboring the diptheria toxin transgene (*NCER**/**R26R-floxDT-A*) were injected with tamoxifen (100 mg/kg body weight) for 10 days starting at 3 weeks of age and analyzed at 7 weeks of age. (B) When quantified, the number of NeuN-positive cells in the CA1 subfield of *NCER**/**R26R-floxDT-A* mice is significantly reduced by 50% when compared with controls ($n = 3$, $P < 0.001$, unpaired, 2 tailed *t*-test with Welch's correction). Scale bars: 20 μ m (FJC); 50 μ m (Map2, NeuN).

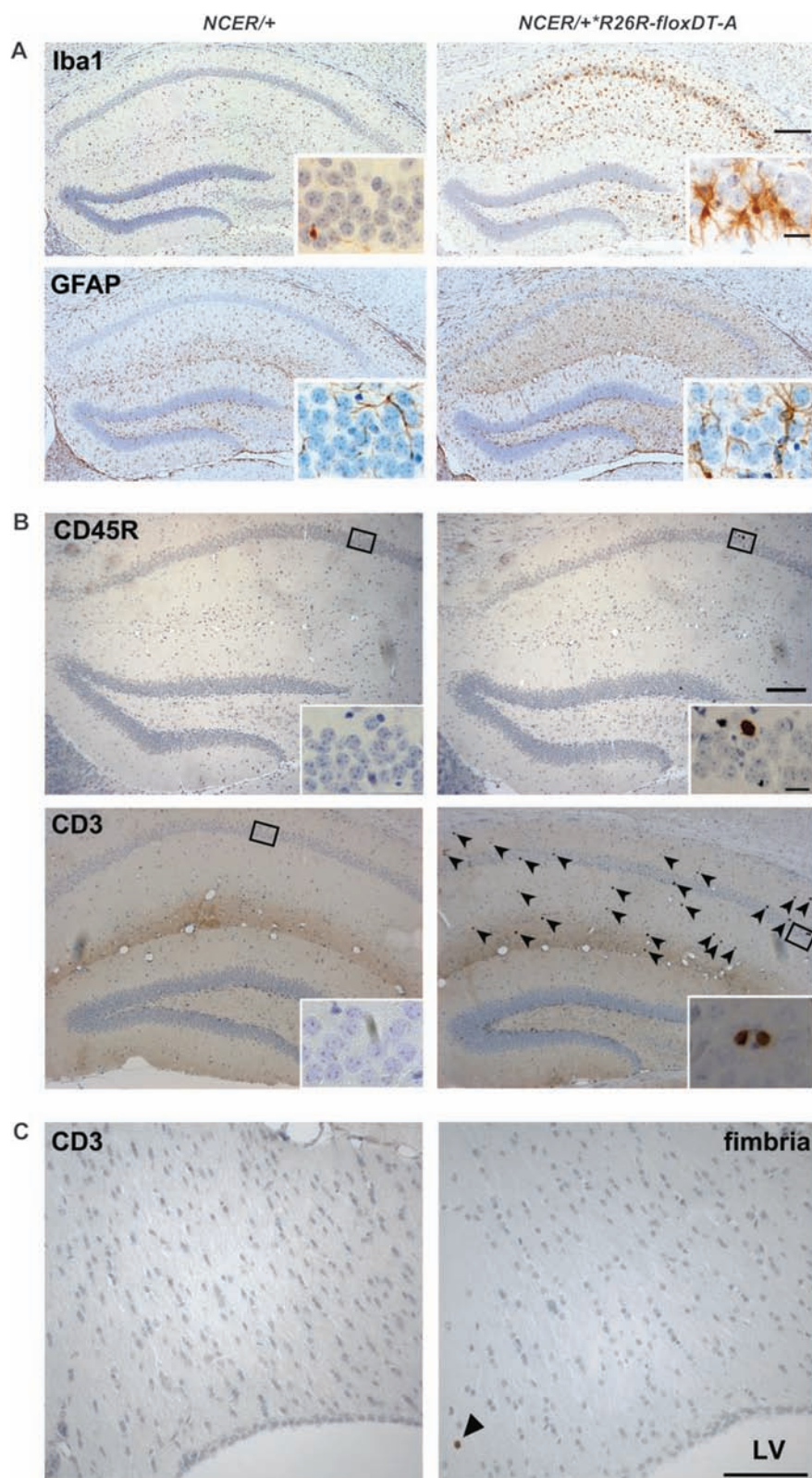


Figure 8. Genetic ablation of hippocampal projection neurons induces reactive gliosis and lymphocyte infiltration. (A) Pyramidal cell death in the hippocampal CA1–3 region of tamoxifen-treated *NCER/+*R26R-floxDT-A* mice is associated with severe microgliosis and astrogliosis as demonstrated by immunostaining for microglia (Iba1, upper panels) and astrocytes (GFAP; lower panels). *NCER/+* controls and *NCER/+*R26R-floxDT-A* mice were injected with tamoxifen for 10 days starting at 4 weeks of age and harvested at 6.5 weeks of age. (B) Lymphocyte infiltration into the hippocampal region of mutant brains shown by immunostaining for B cell-specific phosphatase CD45R (upper panels; magnified in inset) and T cell receptor CD3 (arrows in lower right; magnified in inset). B cells were never observed in brains of control mice. (C) Immunostaining for CD3 demonstrates absence of significant T cell infiltration in hippocampal fimbriae (i.e., myelinated axons derived from degenerating hippocampal neurons) of tamoxifen-treated *NCER/+*R26R-floxDT-A* mice. Arrowhead marks rare example of a T cell infiltrate. Abbreviations: LV, lateral ventricle. Scale bars: 200 μ m (A,B); 20 μ m (insets); 100 μ m (C).

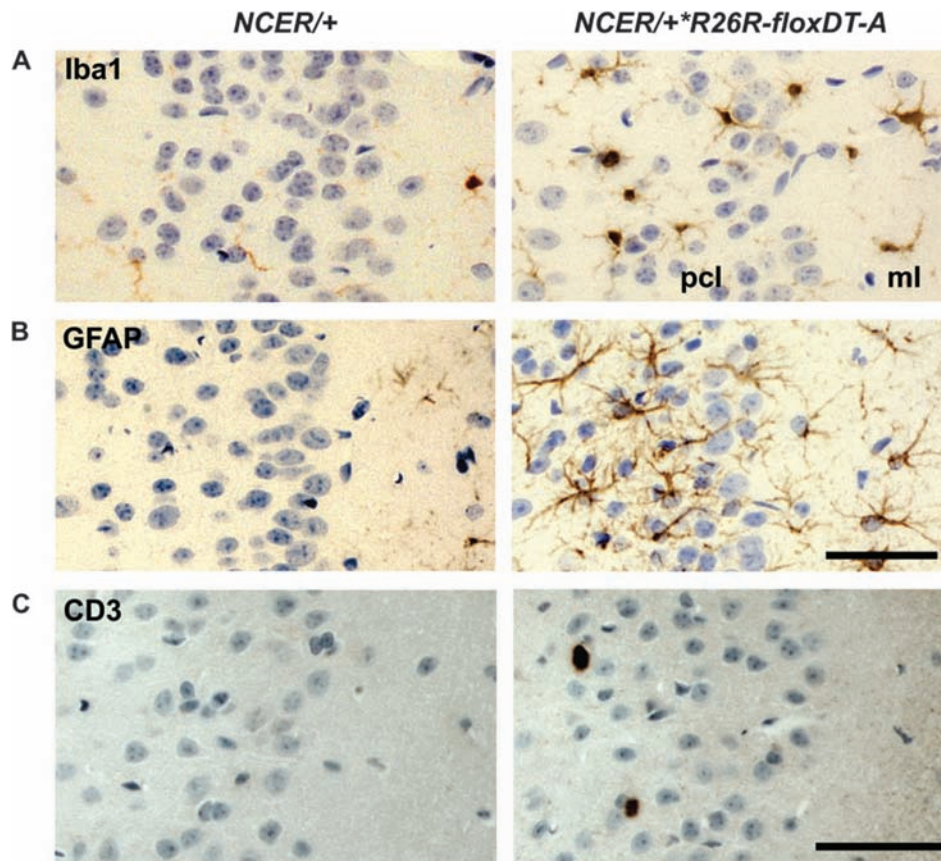


Figure 9. Gliosis and mild T cell infiltration in the cingulate cortex of tamoxifen-treated *NCER/+*R26R-floxDT-A* mice. (A) Immunostaining for Iba1 demonstrates activated microglia as a consequence of DT-A-induced death of pyramidal neurons in the cingulate cortex of tamoxifen-treated *NCER/+*R26R-floxDT-A* mice. (B) Accumulation of reactive astroglia in the cingulate cortex of *NCER/+*R26R-floxDT-A* mice revealed by immunostaining for GFAP. (C) Occasional T cell infiltration in the cingulate cortex of *NCER/+*R26R-floxDT-A* mice as demonstrated by immunostaining for CD3. Note that CD3+ T cells were not observed in the cingulate cortex of tamoxifen-treated *NCER/+* controls. Abbreviations: ml, molecular layer; pcl, pyramidal cell layer. Scale bars: 50 μ m.

(Bormuth and M.H.S. unpublished data). These functions suggest that NEX-positive projection neurons are recruited for distinct plasticity processes in the adult brain, and we speculate that external stimuli dynamically regulate the compartment of NEX-positive neurons in the neocortex. This hypothesis can be further addressed in *NEX-CreERT2* null mutants by combining environmental enrichment paradigms with single-cell transcriptomics, *in vivo* multiphoton imaging, and patch clamp recording.

Classical methods to study individual mammalian neurons, such as dye filling or viral infection, are invasive interventions (Dittgen et al. 2004; Young and Feng 2004). Therefore, strategies for the noninvasive genetic labeling of single neurons have been developed. For example, mosaic analysis with double markers (MADM) makes use of Cre-dependent interchromosomal mitotic recombination to produce small numbers of targeted cells, however, this method is not applicable to postmitotic neurons of the adult brain (Zong et al. 2005). In “SLICK” mice, CreERT2 and EYFP are coexpressed from the same Thy1.2 promoter (Young et al. 2008). Thus, EYFP expression and CreERT2-mediated recombination are not strictly coupled. Sparse cell labeling was achieved by the insertion of CreERT2 coupled to an internal ribosomal entry site into the 3' region of neurally expressed genes, at least when combined with a reporter locus of low recombination efficiency (Rotolo et al. 2008). Placing CreERT2 under control

of regulatory sequences from the CaMKII α gene results in highly efficient recombination in forebrain projection neurons (Erdmann et al. 2007), but if sparse recombination can be achieved was not addressed.

Due to the temporal and spatial expression pattern of the *Nex1* locus, *NEX-CreERT2* mice present a unique tool to perform single-cell genetics in individual cortical projection neurons. Limiting tamoxifen treatment to 2 days allows visualization of complex neuronal arbors, for example, by breeding to a human placental alkaline phosphatase reporter (Lobe et al. 1999). Short-term tamoxifen treatment also produces sparse recombination in CA1–3 pyramidal cells, which can be tested singly as well. Furthermore, *NEX-CreERT2* mice provide the opportunity to address reciprocal interactions between individual projection neurons and other neural cells by breeding to novel CreERT2-dependent fluorescent reporter mice (Madisen et al. 2010) and a variety of other transgenic mouse lines, such as BAC transgenic lines from the GENSAT collection (Gong et al. 2003), lines that express calcium, chloride, and zinc sensors (Kuner and Augustine 2000; Griesbeck 2004; Vinkenborg et al. 2009) or the transsynaptic marker wheat germ agglutinin (Yoshihara et al. 1999).

NEX-CreERT2 mice are also unique with respect to CreERT2 expression in cells of the hippocampal hilar region (most likely glutamatergic mossy cells; Henze and Buzsaki 2007) and indusium griseum, a dorsal portion of the hippocampus, which

contains granule cells, pyramidal cells, and associated white matter (Wyss and Sripanidkulchai 1983; Adamek et al. 1984). Mossy cells and hilar interneurons are connected through reciprocal local circuit networks (Larimer and Strowbridge 2008), and computational modeling suggests a role for hilar cells in pattern separation in the dentate gyrus (Myers and Scharfman 2009), but little is known about the functions of these cells *in vivo*. As adult-born granule cells establish new glutamatergic synapses with hilar interneurons and mossy cells (Toni et al. 2008), genetic manipulation of mossy cells in *NEX-CreERT2* mice provides a novel means to study synaptogenesis in the adult brain. Similarly, the exact function of the indusium griseum has not been addressed *in vivo*. The indusium griseum has been shown to be resistant to neuronal cell loss during aging (Sturrock 1986) and histopathologic hallmarks of Alzheimer's disease are largely absent from the indusium griseum in postmortem brains of patients suffering from Alzheimer's disease (Lippa et al. 1990; Lippa and Smith 1992). Thus, *NEX-CreERT2* mice provide the opportunity to study molecular mechanisms of neuronal survival under disease conditions.

A Novel Mouse Model of Adult Neurodegeneration

Most animal models of neurodegeneration rely on invasive interventions, for example, brain matter aspiration, mechanical disruption of the blood-brain barrier or stereotactic injections of toxins (Jarrard 2002; Siren et al. 2006; Tseng et al. 2009). These techniques result in widespread damage, are prone to inflammatory side effects, and cannot target specific cell types. Although neurodegenerative diseases can produce massive degeneration, they typically affect selective neuronal populations. For example, in brains of Alzheimer's disease patients, projection neurons in hippocampus and entorhinal cortex are vulnerable to degeneration, whereas interneurons are largely spared (Morrison and Hof 1997). To mimic some of these features, we ablated pyramidal neurons by breeding *NEX-CreERT2* mice to transgenic mice that conditionally express the DT-A fragment (Brockschneider et al. 2004, 2006), which kills cells by inhibiting protein synthesis (Collier 1975; Pappenheimer 1977). By tamoxifen treatment of adult *NCER/+R26R-floxDT-A* double transgenic mice, we were able to specifically ablate hippocampal pyramidal neurons (and individual projection neurons in the neocortex) without affecting interneurons or glial cells. As tamoxifen treatment is compatible with behavioral phenotyping (Vogt et al. 2008), such an experimental paradigm will also allow to evaluate the role of these cells in cognitive functions before and after pyramidal neuron-restricted toxin expression.

Noninvasive Ablation of Neurons Causes T Cell Invasion

An unexpected finding, following the ablation of hippocampal neurons by tamoxifen-induced DT-A expression, was the invasion of T cell receptor (CD3)-positive lymphocytes into the brain parenchyma. We note that 2 conceptually related studies, reporting the ablation of oligodendrocytes by expression of the same toxin, failed to trigger any T cell response, despite widespread oligodendrocyte death (Traka et al. 2010; Pohl et al. 2011), even following additional proinflammatory manipulations (A Waisman, B Becher, personal communication). These negative findings contrast with the infiltration of CD8+ T cells in mouse mutants carrying defects that perturb but do not kill oligodendrocytes (Ip et al. 2006; Kassmann et al.

2007). This suggests that T cell infiltration is triggered by injured and live (but not dead) oligodendrocytes. One possible explanation for the massive lymphocyte invasion in our study is a higher level of inflammatory signals originating from ablated neurons compared with ablated oligodendrocytes. Alternatively, gray matter areas might lack anti-inflammatory mechanisms that protect white matter from immune cell invasion. The latter could be relevant for diseases, such as multiple sclerosis, in which the protection from immune invasion fails. We cannot exclude the theoretical possibility that neuronal ablation causes an unspecific opening of the blood-brain barrier. However, the very restricted localization of blood-derived lymphocytes to sites of highest recombination frequency argues against a general breakdown of blood-brain barrier functions.

In conclusion, *NEX-CreERT2* mice will be a valuable tool for studying genetic functions in mature cortical and hippocampal neurons *in vivo*, for neuroimaging at the single-cell level, and for ablating single cortical and hippocampal neurons to study the consequences of acute neurodegeneration in the adult brain.

Supplementary Material

Supplementary material can be found at: <http://www.cercor.oxfordjournals.org/>

Funding

A.A. is supported by a Postdoctoral Fellowship from the National Multiple Sclerosis Society. M.H.S. and K.A.N. acknowledge grant support from the Deutsche Forschungsgemeinschaft (DFG Research Center Molecular Physiology of the Brain, CMPB). K.A.N. holds an ERC Advanced Investigator Grant.

Notes

We thank U. Bode for help with ES cell culture, M. Schindler for blastocyst injections, and C. Casper, D. Flemming, and I. Malade for help with animal husbandry. We also thank A. Fahrenholz and M. Floerl for help with histology. We like to thank D. Riethmacher for providing floxDT-A mice, J. Robbins for CAG-CAT*EGFP mice, and F. Kirchhoff for GFAP-CreERT2 mice. We thank I. Bormuth, A. Saab, and members of the Department of Neurogenetics for helpful discussions. Authors' contribution: A.A., M.H.S., and K.A.N. designed the study, drafted, and wrote the manuscript. A.A. cloned gene-targeting constructs, generated *NEX-CreERT2* mice, and planned all the experiments. A.A. carried out histology, imaging, and noninvasive cell ablation experiments as well as analyzed data. P.D. helped with *in vivo* multiphoton recordings. C.M.K. contributed in histological staining. S.G. provided *Nex1* gene fragments to clone targeting construct. All authors read and approved the final manuscript. *Conflict of Interest*: None declared.

References

- Adamek GD, Shipley MT, Sanders MS. 1984. The indusium griseum in the mouse: architecture, Timm's histochemistry and some afferent connections. *Brain Res Bull.* 12:657-668.
- Bartholoma A, Nave KA. 1994. NEX-1: a novel brain-specific helix-loop-helix protein with autoregulation and sustained expression in mature cortical neurons. *Mech Dev.* 48:217-228.
- Brockschneider D, Lappe-Siefke C, Goebels S, Boesl MR, Nave KA, Riethmacher D. 2004. Cell depletion due to diphtheria toxin fragment A after Cre-mediated recombination. *Mol Cell Biol.* 24:7636-7642.
- Brockschneider D, Pechmann Y, Sonnenberg-Riethmacher E, Riethmacher D. 2006. An improved mouse line for Cre-induced cell ablation due to diphtheria toxin A, expressed from the Rosa26 locus. *Genesis.* 44:322-327.

- Burns KA, Ayoub AE, Breunig JJ, Adhmi F, Weng WL, Colbert MC, Rakic P, Kuan CY. 2007. Nestin-CreER mice reveal DNA synthesis by nonapoptotic neurons following cerebral ischemia hypoxia. *Cereb Cortex*. 17:2585-2592.
- Campsall KD, Mazerolle CJ, De Repentigny Y, Kothary R, Wallace VA. 2002. Characterization of transgene expression and Cre recombinase activity in a panel of Thy-1 promoter-Cre transgenic mice. *Dev Dyn*. 224:135-143.
- Collier RJ. 1975. Diphtheria toxin: mode of action and structure. *Bacteriol Rev*. 39:54-85.
- Danielian PS, Muccino D, Rowitch DH, Michael SK, McMahon AP. 1998. Modification of gene activity in mouse embryos in utero by a tamoxifen-inducible form of Cre recombinase. *Curr Biol*. 8:1323-1326.
- DeFelipe J, Farinas I. 1992. The pyramidal neuron of the cerebral cortex: morphological and chemical characteristics of the synaptic inputs. *Prog Neurobiol*. 39:563-607.
- Dittgen T, Nimmerjahn A, Komai S, Licznarski P, Waters J, Margrie TW, Helmchen F, Denk W, Brecht M, Osten P. 2004. Lentivirus-based genetic manipulations of cortical neurons and their optical and electrophysiological monitoring in vivo. *Proc Natl Acad Sci U S A*. 101:18206-18211.
- Erdmann G, Schutz G, Berger S. 2007. Inducible gene inactivation in neurons of the adult mouse forebrain. *BMC Neurosci*. 8:63.
- Erdmann G, Schutz G, Berger S. 2008. Loss of glucocorticoid receptor function in the pituitary results in early postnatal lethality. *Endocrinology*. 149:3446-3451.
- Feil R, Wagner J, Metzger D, Chambon P. 1997. Regulation of Cre recombinase activity by mutated estrogen receptor ligand-binding domains. *Biochem Biophys Res Commun*. 237:752-757.
- Goebbels S, Bormuth I, Bode U, Hermanson O, Schwab MH, Nave KA. 2006. Genetic targeting of principal neurons in neocortex and hippocampus of NEX-Cre mice. *Genesis*. 44:611-621.
- Gong S, Zheng C, Doughty ML, Losos K, Didkovsky N, Schambra UB, Nowak NJ, Joyner A, Leblanc G, Hatten ME, et al. 2003. A gene expression atlas of the central nervous system based on bacterial artificial chromosomes. *Nature*. 425:917-925.
- Gorski JA, Talley T, Qiu M, Puelles L, Rubenstein JL, Jones KR. 2002. Cortical excitatory neurons and glia, but not GABAergic neurons, are produced in the Emx1-expressing lineage. *J Neurosci*. 22:6309-6314.
- Griesbeck O. 2004. Fluorescent proteins as sensors for cellular functions. *Curr Opin Neurobiol*. 14:636-641.
- Griffiths I, Klugmann M, Anderson T, Yool D, Thomson C, Schwab MH, Schneider A, Zimmermann F, McCulloch M, Nadon N, et al. 1998. Axonal swellings and degeneration in mice lacking the major proteolipid of myelin. *Science*. 280:1610-1613.
- Henze DA, Buzsaki G. 2007. Hilar mossy cells: functional identification and activity in vivo. *Prog Brain Res*. 163:199-216.
- Hirrlinger PG, Scheller A, Braun C, Hirrlinger J, Kirchhoff F. 2006. Temporal control of gene recombination in astrocytes by transgenic expression of the tamoxifen-inducible DNA recombinase variant CreERT2. *Glia*. 54:11-20.
- Horton RM. 1995. PCR-mediated recombination and mutagenesis. SOEing together tailor-made genes. *Mol Biotechnol*. 3:93-99.
- Horton RM. 1997. In vitro recombination and mutagenesis of DNA. SOEing together tailor-made genes. *Methods Mol Biol*. 67:141-149.
- Ip CW, Kroner A, Bendszus M, Leder C, Kobsar I, Fischer S, Wiendl H, Nave KA, Martini R. 2006. Immune cells contribute to myelin degeneration and axonopathic changes in mice overexpressing proteolipid protein in oligodendrocytes. *J Neurosci*. 26:8206-8216.
- Jarrard LE. 2002. Use of excitotoxins to lesion the hippocampus: update. *Hippocampus*. 12:405-414.
- Jordan VC, Murphy CS. 1990. Endocrine pharmacology of antiestrogens as antitumor agents. *Endocr Rev*. 11:578-610.
- Kassmann CM, Lappe-Siefke C, Baes M, Brugger B, Mildner A, Werner HB, Natt O, Michaelis T, Prinz M, Frahm J, et al. 2007. Axonal loss and neuroinflammation caused by peroxisome-deficient oligodendrocytes. *Nat Genet*. 39:969-976.
- Kassmann CM, Nave KA. 2008. Oligodendroglial impact on axonal function and survival—a hypothesis. *Curr Opin Neurol*. 21:235-241.
- Kasthuri N, Lichtman JW. 2007. The rise of the 'projectome'. *Nat Methods*. 4:307-308.
- Kume H, Maruyama K, Tomita T, Iwatsubo T, Saido TC, Obata K. 1996. Molecular cloning of a novel basic helix-loop-helix protein from the rat brain. *Biochem Biophys Res Commun*. 219:526-530.
- Kuner T, Augustine GJ. 2000. A genetically encoded ratiometric indicator for chloride: capturing chloride transients in cultured hippocampal neurons. *Neuron*. 27:447-459.
- Kwon CH, Zhou J, Li Y, Kim KW, Hensley LL, Baker SJ, Parada LF. 2006. Neuron-specific enolase-cre mouse line with cre activity in specific neuronal populations. *Genesis*. 44:130-135.
- Lappe-Siefke C, Goebbels S, Gravel M, Nicksch E, Lee J, Braun PE, Griffiths IR, Nave KA. 2003. Disruption of Cnp1 uncouples oligodendroglial functions in axonal support and myelination. *Nat Genet*. 33:366-374.
- Larimer P, Strowbridge BW. 2008. Nonrandom local circuits in the dentate gyrus. *J Neurosci*. 28:12212-12223.
- Leone DP, Genoud S, Atanasoski S, Grausenburger R, Berger P, Metzger D, Macklin WB, Chambon P, Suter U. 2003. Tamoxifen-inducible glia-specific Cre mice for somatic mutagenesis in oligodendrocytes and Schwann cells. *Mol Cell Neurosci*. 22:430-440.
- Lippa CF, Smith TW. 1992. The indusium griseum in Alzheimer's disease: an immunocytochemical study. *J Neurol Sci*. 111:39-45.
- Lippa CF, Smith TW, Degirolami U, Drachman DA. 1990. The indusium griseum: is it involved in Alzheimer's disease? *Neurobiol Aging*. 11:551-554.
- Lobe CG, Koop KE, Kreppner W, Lomeli H, Gertsenstein M, Nagy A. 1999. Z/AP, a double reporter for cre-mediated recombination. *Dev Biol*. 208:281-292.
- Madisen L, Zwingman TA, Sunkin SM, Oh SW, Zariwala HA, Gu H, Ng LL, Palmiter RD, Hawrylycz MJ, Jones AR, et al. 2010. A robust and high-throughput Cre reporting and characterization system for the whole mouse brain. *Nat Neurosci*. 13:133-140.
- Metzger D, Chambon P. 2001. Site- and time-specific gene targeting in the mouse. *Methods*. 24:71-80.
- Minichiello L, Calella AM, Medina DL, Bonhoeffer T, Klein R, Korte M. 2002. Mechanism of TrkB-mediated hippocampal long-term potentiation. *Neuron*. 36:121-137.
- Mori T, Tanaka K, Buffo A, Wurst W, Kuhn R, Gotz M. 2006. Inducible gene deletion in astroglia and radial glia—a valuable tool for functional and lineage analysis. *Glia*. 54:21-34.
- Morrison JH, Hof PR. 1997. Life and death of neurons in the aging brain. *Science*. 278:412-419.
- Muzumdar MD, Tasic B, Miyamichi K, Li L, Luo L. 2007. A global double-fluorescent Cre reporter mouse. *Genesis*. 45:593-605.
- Myers CE, Scharfman HE. 2009. A role for hilar cells in pattern separation in the dentate gyrus: a computational approach. *Hippocampus*. 19:321-337.
- Nakamura T, Colbert MC, Robbins J. 2006. Neural crest cells retain multipotential characteristics in the developing valves and label the cardiac conduction system. *Circ Res*. 98:1547-1554.
- Nave KA. 2010. Myelination and support of axonal integrity by glia. *Nature*. 468:244-252.
- Nieuwenhuys R. 1994. The neocortex. An overview of its evolutionary development, structural organization and synaptology. *Anat Embryol (Berl)*. 190:307-337.
- Pappenheimer AM, Jr. 1977. Diphtheria toxin. *Annu Rev Biochem*. 46:69-94.
- Pohl HB, Porcheri C, Mueggler T, Bachmann LC, Martino G, Riethmacher D, Franklin RJ, Rudin M, Suter U. 2011. Genetically induced adult oligodendrocyte cell death is associated with poor myelin clearance, reduced remyelination, and axonal damage. *J Neurosci*. 31:1069-1080.
- Rodriguez CI, Buchholz F, Galloway J, Sequerra R, Kasper J, Ayala R, Stewart AF, Dymecki SM. 2000. High-efficiency deleter mice show that FLPe is an alternative to Cre-loxP. *Nat Genet*. 25:139-140.

- Rotolo T, Smallwood PM, Williams J, Nathans J. 2008. Genetically-directed, cell type-specific sparse labeling for the analysis of neuronal morphology. *PLoS One*. 3:e4099.
- Schwab MH, Bartholomae A, Heimrich B, Feldmeyer D, Druffel-Augustin S, Goebbels S, Naya FJ, Zhao S, Frotscher M, Tsai MJ, et al. 2000. Neuronal basic helix-loop-helix proteins (NEX and BETA2/Neuro D) regulate terminal granule cell differentiation in the hippocampus. *J Neurosci*. 20:3714-3724.
- Schwab MH, Druffel-Augustin S, Gass P, Jung M, Klugmann M, Bartholomae A, Rossner MJ, Nave KA. 1998. Neuronal basic helix-loop-helix proteins (NEX, neuroD, NDRF): spatiotemporal expression and targeted disruption of the NEX gene in transgenic mice. *J Neurosci*. 18:1408-1418.
- Siren AL, Radyushkin K, Boretius S, Kammer D, Riechers CC, Natt O, Sargin D, Watanabe T, Sperling S, Michaelis T, et al. 2006. Global brain atrophy after unilateral parietal lesion and its prevention by erythropoietin. *Brain*. 129:480-489.
- Soriano P. 1999. Generalized lacZ expression with the ROSA26 Cre reporter strain. *Nat Genet*. 21:70-71.
- Spruston N. 2008. Pyramidal neurons: dendritic structure and synaptic integration. *Nat Rev Neurosci*. 9:206-221.
- Srinivas S, Watanabe T, Lin CS, William CM, Tanabe Y, Jessell TM, Costantini F. 2001. Cre reporter strains produced by targeted insertion of EYFP and ECFP into the ROSA26 locus. *BMC Dev Biol*. 1:4.
- Sturrock RR. 1986. A quantitative histological study of the indusium griseum and neostriatum in elderly mice. *J Anat*. 149:195-203.
- Toni N, Laplagne DA, Zhao C, Lombardi G, Ribak CE, Gage FH, Schinder AF. 2008. Neurons born in the adult dentate gyrus form functional synapses with target cells. *Nat Neurosci*. 11:901-907.
- Traka M, Arasi K, Avila RL, Podojil JR, Christakos A, Miller SD, Soliven B, Popko B. 2010. A genetic mouse model of adult-onset, pervasive central nervous system demyelination with robust remyelination. *Brain*. 133:3017-3029.
- Tronche F, Kellendonk C, Kretz O, Gass P, Anlag K, Orban PC, Bock R, Klein R, Schutz G. 1999. Disruption of the glucocorticoid receptor gene in the nervous system results in reduced anxiety. *Nat Genet*. 23:99-103.
- Tseng KY, Chambers RA, Lipska BK. 2009. The neonatal ventral hippocampal lesion as a heuristic neurodevelopmental model of schizophrenia. *Behav Brain Res*. 204:295-305.
- Vinkenborg JL, Nicolson TJ, Bellomo EA, Koay MS, Rutter GA, Merkx M. 2009. Genetically encoded FRET sensors to monitor intracellular Zn²⁺ homeostasis. *Nat Methods*. 6:737-740.
- Vogt MA, Chourbaji S, Brandwein C, Dormann C, Sprengel R, Gass P. 2008. Suitability of tamoxifen-induced mutagenesis for behavioral phenotyping. *Exp Neurol*. 211:25-33.
- Weber P, Metzger D, Chambon P. 2001. Temporally controlled targeted somatic mutagenesis in the mouse brain. *Eur J Neurosci*. 14:1777-1783.
- Weber T, Bohm G, Hermann E, Schutz G, Schonig K, Bartsch D. 2009. Inducible gene manipulations in serotonergic neurons. *Front Mol Neurosci*. 2:24.
- Wyss JM, Sripanidkulchai K. 1983. The indusium griseum and anterior hippocampal continuation in the rat. *J Comp Neurol*. 219:251-272.
- Yasunami M, Suzuki K, Maruyama H, Kawakami H, Nagai Y, Hagiwara M, Ohkubo H. 1996. Molecular cloning and characterization of a cDNA encoding a novel basic helix-loop-helix protein structurally related to Neuro-D/BHF1. *Biochem Biophys Res Commun*. 220:754-758.
- Yin X, Baek RC, Kirschner DA, Peterson A, Fujii Y, Nave KA, Macklin WB, Trapp BD. 2006. Evolution of a neuroprotective function of central nervous system myelin. *J Cell Biol*. 172:469-478.
- Yoshihara Y, Mizuno T, Nakahira M, Kawasaki M, Watanabe Y, Kagamiyama H, Jishage K, Ueda O, Suzuki H, Tabuchi K, et al. 1999. A genetic approach to visualization of multisynaptic neural pathways using plant lectin transgene. *Neuron*. 22:33-41.
- Young P, Feng G. 2004. Labeling neurons in vivo for morphological and functional studies. *Curr Opin Neurobiol*. 14:642-646.
- Young P, Qiu L, Wang D, Zhao S, Gross J, Feng G. 2008. Single-neuron labeling with inducible Cre-mediated knockout in transgenic mice. *Nat Neurosci*. 11:721-728.
- Zong H, Espinosa JS, Su HH, Muzumdar MD, Luo L. 2005. Mosaic analysis with double markers in mice. *Cell*. 121:479-492.